Structural Engineering and Mechanics, *Vol. 62, No. 3 (2017) 345-355*
DOI: https://doi.org/10.12989/sem.2017.62.3.345

Free vibration analysis of cracked thin plates using generalized differential quadrature element method

Hossein Shahverdi* and Mohammad M. Navardi

Department of Aerospace Engineering and Center of Excellence in Computational Aerospace, Amirkabir University of Technology, 424 Hafez Avenue, Tehran 15875-4413, Iran

(Received July 26, 2016, Revised February 14, 2017, Accepted February 15, 2017)

Abstract. The aim of the present study is to develop an elemental approach based on the differential quadrature method for free vibration analysis of cracked thin plate structures. For this purpose, the equations of motion are established using the classical plate theory. The well-known Generalized Differential Quadrature Method (GDQM) is utilized to discretize the governing equations on each computational subdomain or element. In this method, the differential terms of a quantity field at a specific computational point should be expressed in a series form of the related quantity at all other sampling points along the domain. However, the existence of any geometric discontinuity, such as a crack, in a computational domain causes some problems in the calculation of differential terms. In order to resolve this problem, the multi-block or elemental strategy is implemented to divide such geometry into several subdomains. By constructing the appropriate continuity conditions at each interface between adjacent elements and a crack tip, the whole discretized governing equations of the structure can be established. Therefore, the free vibration analysis of a cracked thin plate will be provided via the achieved eigenvalue problem. The obtained results show a good agreement in comparison with those found by finite element method.

Keywords: continuity condition; crack; differential quadrature method; element; thin plate

1. Introduction

Thin flat plates are known as a major component and widely used in various industries such as mechanical, civil and aerospace. The emergence of a crack in this type of structures results in a reduction of the local stiffness and the strength of them. It is obvious that changing the stiffness of a structure is caused to change its natural frequencies which lead to a different structural dynamics behavior. Hence, investigation of the structural behavior due to the presence of a crack in a structure is very attractive for scientists.

Many physical problems such as the free vibration analysis of thin cracked plates are expressed by partial differential equations. The solution of these equations is generally very difficult and often impossible to obtain via analytical means. Hence, it is inevitable to use numerical methods, such as FEM, Raleigh-Ritz,… (Bachene 2009, Huang 2009, 2011, Israr 2008, Bose 2013), to overcome this problem. However, the methods which have high accuracy, as well as low computational effort, are more attractive. In recent decades, some numerical tools such as mesh-free method, boundary element method, and DQM, have been developed to provide a solution of the aforementioned problem.

The DQ method, which was first developed by Bellman and Casti (1971), has less complexity than other numerical methods in solving partial differential equations in simple domains. In this method, the derivative of a quantity field at a specific point is approximated as a weighted linear summation of the values of the quantity at all other sampling points along the domain. Of course, the main drawbacks of this method are (i) sensitive to distribution type of sampling points along the domain, and (ii) the existence of a geometric discontinuity or complexity in a computational domain. Therefore, Shu and Richards (1992) proposed a method to overcome the first drawback by introducing the Generalized DQ (GDQ) method based on the analysis of a polynomial vector space. Afterward, many researchers used this method for analyzing different problems containing partial differential equations in 2D and 3D problems. For example, Chen *et al*. (1997) introduced a methodology to implement the boundary conditions in the DQ solution of plate and beam problems. Also, the DQ method was used to solve the Poisson and Convection-Diffusion Equations (Chen *et al*. 2002). However, the structural analysis of a plate structure with geometric and material discontinuity/complexity is impossible by using ordinary DQ or GDQ method. One way to vanish this problem is to use the Differential Quadrature Element Method (DQEM) (Striz *et al*. 1994). In this method, a computational domain is divided into several sub-domains (elements) which joined together mathematically by continuity conditions. The DQEM approach was utilized to analyze the free vibration of cracked beams and some its excellent features such as high accuracy and fast convergence were introduced (Hsu 1995, Ke *et al*. 2012, Torabi 2014). Also, Han and Liu (1996) presented a DQE method for partly thick plates. In another study, this method was implemented by Liu (1999) to investigate the vibration

∗Corresponding author, Assistant Professor
E-mail: h_shahverdi@aut.ac.ir

ISSN: 1225-4568 (Print), 1598-6217 (Online)

analysis of a discontinuous Mindlin's plate. Also, this method was applied to investigate the buckling, free vibration and static analyses of discontinuous Mindlin's plates (Liu 1998, 1999a, b, 2001). Barooti *et al*. (2013) examined the effects of a through-the-width delamination on the buckling load of a laminated composite partly thick plate subjected to a compressive load by DQEM approach. Although the appropriate application of this approach has been proven in analyzing of beam and thick plate structures, it has some restrictions on dealing with thin plates. A simplified approach to analyze thin plate structures is the use of classical plate theory (the Kirchhoff–Love theory of plates) which may lead to partial differential equations including only deflection degree of freedom. However, the resultant equations cannot provide enough means for imposing boundary conditions and continuity conditions between elements via DQE method. Thus, it is inevitable to implement some correction techniques to overcome this drawback. In this regard, various approaches have been proposed to solve the problem of imposing boundary conditions in a thin plate structure by DQE method. However, these approaches have some restrictions such as they are regardless of enough boundary condition relations or the related equations in the vicinity of boundaries. To resolve this problem, many researchers have considered additional degrees of freedom at the boundary of a computational domain (element) to facilitate applying boundary or continuity conditions. For example, Wu and Liu (2001) defined a slope degree of freedom at the boundary of a domain via a change in the weighting coefficients appears in the equivalent statement of a partial derivative. They performed the static and dynamic analyses of an Euler-Bernoulli beam and a rectangular plate under different boundary conditions. Also, Wang *et al*. (2004) implied that the application of this routine in the DQEM is not suitable for a problem having discontinuities. Karami and Malekzadeh (2003) proposed curvature degrees of freedom at the boundary of a problem without any change in the weighting coefficient statements of GDQ method and investigated the free vibration behavior of a thin rectangular plate. However, this technique is not appropriate for the structural analysis of a problem having geometric discontinuity because of the insufficient degrees of freedom at corner points of each computational domain. Moreover, it has some drawbacks in applying slope boundary conditions (Navardi 2015). In another study, Wang *et al*. proposed slope degrees of freedom at the boundary of a problem to provide a manner to apply slope type of boundary conditions in GDQ method. However, in this approach, the related weighing coefficients remain unchanged. Despite a corner point of a domain in this approach has three degrees of freedom (one deformation along with two slopes), the slope degrees of freedom are not present in the twist statement. Although this approach may not be faced with any problem in continuous domains; however, it is not appropriate to model cracked or cutout thin plates.

Fantuzzi (2013) introduced the generalized differential quadrature finite element method. This method was used to investigate the free vibration of arbitrary shaped membranes (Fantuzzi *et al*. 2014) and cracked composite structures of arbitrary shape (Viola *et al*. 2013).They implemented the first-order shear deformation plate theories in their research. Although the presented results show the higher accuracy of this approach, the manner of applying continuity conditions between adjacent DQ elements and boundary conditions has not been explicitly proposed. It is worth mentioning that using the first-order shear deformation removes the need of considering additional degrees of freedom. However, the simplicity of classical plate theory still retains the charm of its use in the analysis of thin plate structures.

In the present study, an alternative approach based on the Generalized Differential Quadrature Element (GDQE) method is developed to overcome the establishment of continuity between adjacent DQ elements and simulating thin plate structures with geometric discontinuity and mixed boundary conditions. For this purpose, the slope degree of freedom as an independent variable is introduced on the boundaries of a DQ element by modifying the governing differential equation so that three degrees of freedom are produced at each corner point. It should be noted that the present approach is similar to the new version of the differential quadrature element method, has been introduced by Wang *et al*. (2004), which may be lead to an ill-conditioned problem during the analysis of a plate with clamped boundary conditions. Finally, the present approach is utilized to free vibration analysis of thin cracked plate structures. The obtained results are evaluated with the available results in the literature.

2. Governing equations

The governing equation of a thin plate, with length (*a*), width (*b*) and thickness (h), based on the classical plate theory and regardless of surface shearing forces, body moments and inertial forces in *x* and *y*-direction is (Reddy 2004)

$$\frac{\partial^2 M_{xx}}{\partial x^2}+2\frac{\partial^2 M_{xy}}{\partial y\,\partial x}+\frac{\partial^2 M_{yy}}{\partial y^2}+N(w_0)+q=I_0\frac{\partial^2 w_0}{\partial t^2} \quad (1)$$

Also

$$\begin{aligned} &I_0=\int_{-h/2}^{h/2}\rho(z)dz \quad , \\ &N(w_0)=\frac{\partial}{\partial x}(\mathrm{N}_{xx}\frac{\partial w_0}{\partial x}+N_{xy}\frac{\partial w_0}{\partial y})+ \\ &\frac{\partial}{\partial y}(\mathrm{N}_{xy}\frac{\partial w_0}{\partial x}+N_{yy}\frac{\partial w_0}{\partial y}) \end{aligned} \quad (2)$$

where M_{xx}, M_{yy} and M_{xy} denote the components of out-of-plate moment. q and ρ denote the intensity of transverse distributed load and the plate mass density per unit area, respectively. N_{xx}, N_{yy} and N_{xy} are the component of in-plane forces. Also, w_0 and I_0 are the transverse displacement and the plate's mass moment of inertia.

Based on the classical plate theory, the displacement field of a plate is as follows

$$u(x,y,z,t)=u_0(x,y,t)-z\,\frac{\partial w_0(x,y,t)}{\partial x}$$
$$v(x,y,z,t)=v_0(x,y,t)-z\,\frac{\partial w_0(x,y,t)}{\partial y} \tag{3}$$
$$w(x,y,z,t)=w_0(x,y,t)$$

where u, v and w are the displacement component in the x, y and z directions, respectively. u_0 and v_0 are the in-plane displacement components, and w_0 is the out-of-plane displacement component of the mid-plane of the plate.

According to von Karman nonlinear strain-displacement relations, the nonlinear strains are defined as

$$\{\varepsilon\}=\{\varepsilon^0\}+z\,\{k\} \tag{4}$$

where ε^0 and k are the mid-plane membrane and bending strain vectors

$$\{\varepsilon^0\}=\begin{Bmatrix}\varepsilon_{xx}{}^0\\ \varepsilon_{yy}{}^0\\ \varepsilon_{xy}{}^0\end{Bmatrix}=\begin{Bmatrix}\dfrac{\partial u_0}{\partial x}\\ \dfrac{\partial v_0}{\partial y}\\ \dfrac{\partial u_0}{\partial y}+\dfrac{\partial v_0}{\partial x}\end{Bmatrix}+\frac{1}{2}\begin{Bmatrix}\left(\dfrac{\partial w_0}{\partial x}\right)^2\\ \left(\dfrac{\partial w_0}{\partial y}\right)^2\\ 2\dfrac{\partial w_0}{\partial x}.\dfrac{\partial w_0}{\partial y}\end{Bmatrix} \tag{5}$$

The curvatures are also defined by

$$\begin{Bmatrix}k_x\\ k_y\\ k_{xy}\end{Bmatrix}=\begin{Bmatrix}\dfrac{\partial}{\partial x}\left(\dfrac{\partial w_0}{\partial x}\right)\\ \dfrac{\partial}{\partial y}\left(\dfrac{\partial w_0}{\partial y}\right)\\ \dfrac{\partial}{\partial x}\left(\dfrac{\partial w_0}{\partial y}\right)+\dfrac{\partial}{\partial y}\left(\dfrac{\partial w_0}{\partial x}\right)\end{Bmatrix} \tag{6}$$

The out-of-plane moments are related to the curvatures through the following relations

$$\{\varepsilon^0\}=\begin{Bmatrix}\varepsilon_{xx}{}^0\\ \varepsilon_{yy}{}^0\\ \varepsilon_{xy}{}^0\end{Bmatrix}=\begin{Bmatrix}\dfrac{\partial u_0}{\partial x}\\ \dfrac{\partial v_0}{\partial y}\\ \dfrac{\partial u_0}{\partial y}+\dfrac{\partial v_0}{\partial x}\end{Bmatrix}+\frac{1}{2}\begin{Bmatrix}\left(\dfrac{\partial w_0}{\partial x}\right)^2\\ \left(\dfrac{\partial w_0}{\partial y}\right)^2\\ 2\dfrac{\partial w_0}{\partial x}.\dfrac{\partial w_0}{\partial y}\end{Bmatrix} \tag{7}$$

where D denotes the plate flexural rigidity and is associated with Young's modulus and Poison's ratio via

$$D=\frac{Eh^3}{12(1-\upsilon^2)} \tag{8}$$

The shear force and the total transverse force components are expressed by Viola *et al*. (2013)

$$Q_x=\frac{\partial M_{xx}}{\partial x}+\frac{\partial M_{xy}}{\partial y}$$
$$Q_y=\frac{\partial M_{yy}}{\partial y}+\frac{\partial M_{xy}}{\partial x} \tag{9}$$

$$Q_x=\frac{\partial M_{xx}}{\partial x}+\frac{\partial M_{xy}}{\partial y}$$
$$Q_y=\frac{\partial M_{yy}}{\partial y}+\frac{\partial M_{xy}}{\partial x} \tag{10}$$

In order to introduce a refined approach in the differential quadrature element method, one can make some modifications in the aforementioned relations. So, the transverse displacement derivatives according to the following relationships are firstly considered as

$$\Psi^x=\frac{\partial w_0}{\partial x}\ ,\ \Psi^y=\frac{\partial w_0}{\partial y} \tag{11}$$

By changing the degrees of freedom according to rotations of the normal about x and y-axis, The curvature vector can be rewritten as

$$\begin{Bmatrix}k_x\\ k_y\\ k_{xy}\end{Bmatrix}=\begin{Bmatrix}\dfrac{\partial\Psi^x}{\partial x}\\ \dfrac{\partial\Psi^y}{\partial y}\\ \dfrac{\partial\Psi^y}{\partial x}+\dfrac{\partial\Psi^x}{\partial y}\end{Bmatrix} \tag{12}$$

Also, the out-of-plate moment components are expressed by

$$M_{xx}=D\left(\frac{\partial\Psi^x}{\partial x}+\upsilon\frac{\partial\Psi^y}{\partial y}\right)$$
$$M_{yy}=D\left(\frac{\partial\Psi^y}{\partial y}+\upsilon\frac{\partial\Psi^x}{\partial x}\right) \tag{13}$$
$$M_{xy}=\frac{\mathrm{D}(1-\upsilon)}{2}\left(\frac{\partial\Psi^y}{\partial x}+\frac{\partial\Psi^x}{\partial y}\right)$$

Substituting Eq. (13) into Eq. (1) and neglecting in-plane load, $N(w_0)$, yields

$$D\left(\frac{\partial^3\Psi^x}{\partial x^3}+\frac{\partial^3\Psi^x}{\partial x\,\partial y^2}+\frac{\partial^3\Psi^y}{\partial y\,\partial x^2}+\frac{\partial^3\Psi^y}{\partial y^3}\right)=\frac{\partial^2 w_0}{\partial t^2} \tag{14}$$

Eq. (14) can be written in a non-dimensional form as

$$\left[\frac{\partial^3\psi^x}{\partial\xi^3}+\lambda^2\left(\frac{\partial^3\psi^x}{\partial\xi\partial\eta^2}+\frac{\partial^3\psi^y}{\partial\eta\partial\xi^2}\right)+\lambda^4\frac{\partial^3\psi^y}{\partial\eta^3}\right]=\frac{pha^4}{D}\frac{\partial^2 W}{\partial\tau^2} \tag{15}$$

where the non-dimensional parameters appeared in Eq. (15) are defined as follows

$$\xi=\frac{x}{a}\qquad \eta=\frac{y}{b}$$
$$\psi^x=\frac{\Psi^x}{a}\qquad \psi^y=\frac{\Psi^y}{b} \tag{16}$$
$$W=\frac{w_0}{h}\qquad \tau=t\left(\frac{D}{pha^4}\right)\qquad \lambda=\frac{a}{b}$$

Incorporating $W=we^{i\omega t}$ into Eq. (15) gives

$$\left[\frac{\partial^3\psi^x}{\partial\xi^3}+\lambda^2\left(\frac{\partial^3\psi^x}{\partial\xi\partial\eta^2}+\frac{\partial^3\psi^y}{\partial\eta\partial\xi^2}\right)+\lambda^4\frac{\partial^3\psi^y}{\partial\eta^3}\right]=\Omega^2 w \tag{17}$$

where $\Omega=\sqrt{\frac{pha^4}{D}}\omega$ is the dimensionless natural frequency.

By substituting Eq. (13) into of Eq. (9), the shear force components become

$$
\begin{aligned}
Q_x &= \frac{D}{a^3}\left[\frac{\partial^2\psi^x}{\partial\xi^2}+\left(\frac{1-\upsilon}{2}\lambda^3\right)\frac{\partial^2\psi^x}{\partial\eta^2}+\left(\frac{1+\upsilon}{2}\lambda^2\right)\frac{\partial^2\psi^y}{\partial\xi\partial\eta}\right]\\
Q_y &= \frac{D}{a^3}\left[\lambda^3\frac{\partial^2\psi^y}{\partial\eta^2}+\left(\frac{1-\upsilon}{2}\right)\frac{\partial^2\psi^y}{\partial\xi^2}+\left(\frac{1+\upsilon}{2}\right)\lambda\frac{\partial^2\psi^x}{\partial\xi\partial\eta}\right]
\end{aligned}
\tag{18}
$$

Also, in a similar manner the total transverse force components can be written as follows

$$
\begin{aligned}
V_x &= \frac{D}{a^3}\left[\frac{\partial^2\psi^x}{\partial\xi^2}+(1-\upsilon)\lambda^3\frac{\partial^2\psi^x}{\partial\eta^2}+\lambda^2\frac{\partial^2\psi^y}{\partial\xi\partial\eta}\right]\\
V_y &= \frac{D}{a^3}\left[\lambda^3\frac{\partial^2\psi^y}{\partial\eta^2}+(1-\upsilon)\frac{\partial^2\psi^y}{\partial\xi^2}+\lambda\frac{\partial^2\psi^x}{\partial\xi\partial\eta}\right]
\end{aligned}
\tag{19}
$$

3. Refined differential quadrature element method

In this section, the formulation of the refined conventional DQEM is presented. For this purpose, the governing equation of thin plates in the form of Eq. (15) is firstly discretized by using the GDQ method. The key of this method is to determine the derivative of a function with respect to a space variable at a specific point as a weighted linear summation of all the functional values at all other sampling points along the domain (Shu and Richards 1992). Therefore, the r-th order partial derivative of a function $f(x)$ with respect to the space variable x may be written as

$$\left.\frac{\partial^r f(x)}{\partial x^r}\right|_{x=x_i}=\sum_{k=1}^{N}A_{ik}^{(r)}f_{kj} \tag{20}$$

where N is the number of sampling points in the domain and $A_{ik}^{(r)}$ is the weighting coefficients to be defined as follows (Shu and Richards 1992):

The first-order weighting coefficients are

$$A_{ik}^{(1)}=\begin{cases}\dfrac{\prod(x_i)}{(x_i-x_k)\prod(x_k)} & i\neq k\\ -\displaystyle\sum_{j=1,j\neq i}^{M}A_{ij}^{(1)} & i=k\end{cases} \tag{21}$$

where

$$\Pi(x_i)=\prod_{j=1,j\neq i}^{N}(x_i-x_j)\ \text{ and }\ \Pi(x_k)=\prod_{j=1,j\neq k}^{N}(x_k-x_j) \tag{22}$$

Also, the higher-order weighting coefficients are

$$A_{ik}^{(r)}=\begin{cases}r\left[A_{ii}^{(r-1)}A_{ik}^{(1)}-\dfrac{A_{ik}^{(r-1)}}{x_i-x_k}\right] & i\neq k\\ -\displaystyle\sum_{j=1,j\neq i}^{M}A_{ij}^{(r)} & i=k\end{cases} \tag{23}$$

It should be noted that the weighting coefficients are only dependent on the derivative order and on the number and distribution of sampling points along the domain. A well-known method of defining these points is to use Chebyshev-Gauss-Lobatto point distribution as follows (Shu 2012 and Zong and Zhang 2009)

$$x_i=\frac{1}{2}\left[1-\cos\frac{(i-1)}{(\mathrm{N}-1)}\pi\right],\quad i=1,2,\ldots,N \tag{24}$$

By defining the degrees of freedom slope at the edge of an element and the transverse displacement in all domains; $\frac{\partial\psi^x}{\partial\xi}$ ، $\frac{\partial\psi^y}{\partial\eta}$ ، $\frac{\partial^2\psi^x}{\partial\xi\partial\eta}$ and $\frac{\partial^2\psi^y}{\partial\xi\partial\eta}$ can be expressed in the DQ discretization form as

$$
\begin{aligned}
\frac{\partial\psi^x}{\partial\xi} &= \sum_{k_1=1}^{N}A_{ik_1}^{\xi}\psi_{k_1j}^{x}=A_{i1}^{\xi}\psi_{1j}^{x}+A_{iN}^{\xi}\psi_{Nj}^{x}+\\
&\sum_{k_1=2}^{N-1}\sum_{k_2=1}^{N}A_{ik_1}^{\xi}A_{k_1k_2}^{\xi}w_{k_2j}\\
\frac{\partial\psi^y}{\partial\eta} &= \sum_{k_1=1}^{M}A_{jk_1}^{\eta}\psi_{ik_1}^{y}=A_{j1}^{\eta}\psi_{i1}^{y}+A_{jM}^{\eta}\psi_{iM}^{y}+\\
&\sum_{k_1=2}^{M-1}\sum_{k_2=1}^{M}A_{jk_1}^{\eta}A_{k_1k_2}^{\eta}w_{ik_2}\\
\frac{\partial^2\psi^x}{\partial\xi\partial\eta} &= \sum_{k_1=1}^{N}\sum_{k_2=1}^{M}A_{ik_1}^{\xi}A_{jk_2}^{\eta}\psi_{k_1k_2}^{x}=\sum_{k_2=1}^{M}A_{i1}^{\xi}A_{jk_2}^{\eta}\psi_{1k_2}^{x}\\
&+\sum_{k_2=1}^{M}A_{iN}^{\xi}A_{jk_2}^{\eta}\psi_{Nk_2}^{x}+\sum_{k_1=2}^{N-1}\sum_{k_2=1}^{M}\sum_{k_3=1}^{N}A_{ik_1}^{\xi}A_{jk_2}^{\eta}A_{k_1k_3}^{\xi}w_{k_3k_2}\\
\frac{\partial^2\psi^y}{\partial\xi\partial\eta} &= \sum_{k_1=1}^{N}\sum_{k_2=1}^{M}A_{ik_1}^{\xi}A_{jk_2}^{\eta}\psi_{k_1k_2}^{y}=\sum_{k1=1}^{N}A_{ik_1}^{\xi}A_{j1}^{\eta}\psi_{k_11}^{y}+\\
&\sum_{k_1=1}^{N}A_{ik_1}^{\xi}A_{jM}^{\eta}\psi_{k_1M}^{y}+\sum_{k_1=1}^{N}\sum_{k_2=2}^{M-1}\sum_{k_3=1}^{M}A_{ik_1}^{\xi}A_{jk_2}^{\eta}A_{k_2k_3}^{\eta}w_{k_1k_3}
\end{aligned}
\tag{25}
$$

Although $\frac{\partial^2\psi^x}{\partial\eta^2}$ in Eq. 19 on $\xi=0$ or $\xi=1$ can be expressed by

$$\left.\frac{\partial^2\psi^x}{\partial\eta^2}\right|_{ij}=\sum_{k=1}^{M}B_{jk}^{y}\psi_{ik}^{x}\qquad \text{for } i=1 \text{ and } i=N \tag{26}$$

However, it must be approximated by

$$\sum_{k_1=1}^{M}B_{jk}^{\eta}\psi_{ik}^{x}=B_{j1}^{\eta}\psi_{i1}^{x}+B_{jM}^{\eta}\psi_{iM}^{x}+\sum_{k=2}^{M-1}\sum_{k_1=1}^{N}B_{jk}^{\eta}A_{kk_1}^{\xi}w_{k_1j}\quad \text{for } i=1 \text{ and } i=N \tag{27}$$

where N and M denote the number of computational/ sampling points in ξ and η direction, respectively. In the above equations, it can be seen that there are two and three degrees of freedom at the edges and the corner points of a computational domain (element), respectively, via the equivalent summations of the aforementioned partial derivatives. Also, each of the remaining points (called domain points) has only one degree of freedom. In addition to the presence of transverse displacement degrees of freedom, there are slope degrees of freedom in Eq. (25) which are the difference between the present study and the conventional DQEM (Wang *et al*. 2004).

Substituting the partial derivatives in Eq. (15), in a similar manner of Eq. (25), the following equation will be achieved.

$$\left(C^{\xi}_{i1}\psi^{x}_{1j}+C^{\xi}_{iN}\psi^{x}_{Nj}+\sum_{m=2}^{N-1}\sum_{n=1}^{M}C^{\xi}_{im}A^{\xi}_{mn}w_{nj}\right)+\lambda^4\left(C^{\eta}_{j1}\psi^{y}_{i1}+C^{\eta}_{jM}\psi^{y}_{iM}+\sum_{m=2}^{M-1}\sum_{n=1}^{N}C^{\eta}_{jm}A^{\eta}_{mn}w_{in}\right)+\lambda^2\begin{pmatrix}\sum_{n=1}^{M}A^{\xi}_{i1}B^{\eta}_{jn}\psi^{x}_{1n}+\sum_{n=1}^{M}A^{\xi}_{iN}B^{\eta}_{jn}\psi^{x}_{Nn}+\\ \sum_{m=2}^{N-1}\sum_{n=1}^{M}\sum_{k=1}^{N}A^{\xi}_{im}B^{\eta}_{jn}A^{\xi}_{mk}w_{kn}+\sum_{m=1}^{N}B^{\xi}_{im}A^{\eta}_{j1}\psi^{y}_{m1}+\\ \sum_{m=1}^{N}B^{\xi}_{im}A^{\eta}_{jM}\psi^{y}_{mM}+\sum_{m=1}^{N}\sum_{n=2}^{M-1}\sum_{k=1}^{M}B^{\xi}_{im}A^{\eta}_{jn}A^{\eta}_{nk}w_{mk}\end{pmatrix}=\Omega^2 w_{ij} \tag{28}$$

$$\text{for}\quad 2\le i\le N-1\ \text{and}\ 2\le j\le M-1$$

$$M_{xx}=\frac{D}{a^2}\left[\begin{gathered}\left(A^{\xi}_{i1}\psi^{x}_{1j}+A^{\xi}_{iN}\psi^{x}_{Nj}+\sum_{k_1=2}^{N-1}\sum_{k_2=1}^{N}A^{\xi}_{ik_1}A^{\xi}_{k_1k_2}w_{k_2j}\right)\\ +\upsilon\lambda^2\left(A^{\eta}_{j1}\psi^{y}_{i1}+A^{\eta}_{j1}\psi^{y}_{iM}+\sum_{k_1=2}^{M-1}\sum_{k_2=1}^{M}A^{\eta}_{jk_1}A^{\eta}_{k_1k_2}w_{ik_2}\right)\end{gathered}\right]$$

$$M_{yy}=\frac{D}{a^2}\left[\begin{gathered}\upsilon\lambda^2\left(A^{\eta}_{j1}\psi^{y}_{i1}+A^{\eta}_{j1}\psi^{y}_{iM}+\sum_{k_1=2}^{M-1}\sum_{k_2=1}^{M}A^{\eta}_{jk_1}A^{\eta}_{k_1k_2}w_{ik_2}\right)\\ +\left(A^{\xi}_{i1}\psi^{x}_{1j}+A^{\xi}_{iN}\psi^{x}_{Nj}+\sum_{k_1=2}^{N-1}\sum_{k_2=1}^{N}A^{\xi}_{ik_1}A^{\xi}_{k_1k_2}w_{k_2j}\right)\end{gathered}\right]$$

$$M_{xy}=\frac{D(1-\upsilon)}{2.ab}\left[\begin{gathered}A^{\xi}_{i1}\psi^{y}_{1j}+A^{\xi}_{iN}\psi^{y}_{Nj}+\sum_{k_1=2}^{N-1}\sum_{k_2=1}^{M}A^{\xi}_{ik_1}A^{\eta}_{jk_2}w_{k_1k_2}\\ +A^{\eta}_{j1}\psi^{x}_{i1}+A^{\eta}_{jM}\psi^{x}_{iM}+\sum_{k_1=2}^{M-1}\sum_{k_2=1}^{N}A^{\eta}_{jk_1}A^{\xi}_{ik_2}w_{k_2k_1}\end{gathered}\right]$$

$$\begin{aligned}\frac{Q_x.a^3}{D}&=B^{\xi}_{i1}\psi^{x}_{1j}+B^{\xi}_{iN}\psi^{x}_{Nj}+\sum_{k_1=2}^{N-1}\sum_{k_2=1}^{N}B^{\xi}_{ik_1}A^{\xi}_{k_1k_2}w_{k_2j}+\\ &\frac{(1+\upsilon)}{2}\lambda^2\begin{pmatrix}\sum_{k_1=1}^{N}A^{\xi}_{ik_1}A^{\eta}_{j1}\psi^{y}_{k_11}+\sum_{k_1=1}^{N}A^{\xi}_{ik_1}A^{\eta}_{jM}\psi^{y}_{k_1M}\\ +\sum_{k_1=1}^{N}\sum_{k_2=2}^{M-1}\sum_{k_3=1}^{M}A^{\xi}_{ik_1}A^{\eta}_{jk_2}A^{\eta}_{k_2k_3}w_{k_1k_3}\end{pmatrix}\\ &+\frac{(1-\upsilon)}{2}\lambda^3\begin{pmatrix}B^{\eta}_{j1}\psi^{x}_{i1}+B^{\eta}_{jM}\psi^{x}_{iM}\\ +\sum_{k_1=2}^{M-1}\sum_{k_2=1}^{N}B^{\eta}_{jk_1}A^{\xi}_{ik_2}w_{k_2k_1}\end{pmatrix}\end{aligned}$$

$$\begin{aligned}\frac{Q_y.a^3}{D}&=\lambda^3\left(B^{\eta}_{j1}\psi^{y}_{i1}+B^{\eta}_{jM}\psi^{y}_{iM}+\sum_{k_1=2}^{M-1}\sum_{k_2=1}^{M}B^{\eta}_{jk_1}A^{\eta}_{k_1k_2}w_{ik_2}\right)+\\ &\left(\frac{1+\upsilon}{2}\right)\lambda\begin{pmatrix}\sum_{k_1=1}^{M}A^{\xi}_{i1}A^{\eta}_{jk_1}\psi^{x}_{1k_1}+\sum_{k_1=1}^{M}A^{\xi}_{iM}A^{\eta}_{jk_1}\psi^{x}_{Mk_1}\\ +\sum_{k_1=1}^{N-1}\sum_{k_2=1}^{M}\sum_{k_3=1}^{N}A^{\xi}_{ik_1}A^{\eta}_{jk_2}A^{\xi}_{k_2k_3}w_{k_3k_2}\end{pmatrix}\\ &+\frac{(1-\upsilon)}{2}\begin{pmatrix}B^{\xi}_{i1}\psi^{y}_{1j}+B^{\xi}_{iN}\psi^{y}_{Nj}\\ +\sum_{k_1=2}^{N-1}\sum_{k_2=1}^{M}B^{\xi}_{ik_1}A^{\eta}_{jk_2}w_{k_1k_2}\end{pmatrix}\end{aligned}$$

$$\begin{aligned}\frac{V_x.a^3}{D}&=B^{\xi}_{i1}\psi^{x}_{1j}+B^{\xi}_{iN}\psi^{x}_{Nj}+\sum_{k_1=2}^{N-1}\sum_{k_2=1}^{N}B^{\xi}_{ik_1}A^{\xi}_{k_1k_2}w_{k_2j}+\\ &\lambda^2\begin{pmatrix}\sum_{k1=1}^{N}A^{\xi}_{ik_1}A^{\eta}_{j1}\psi^{y}_{k_11}+\sum_{k_1=1}^{N}A^{\xi}_{ik_1}A^{\eta}_{jM}\psi^{y}_{k_1M}\\ +\sum_{k_1=1}^{N}\sum_{k_2=2}^{M-1}\sum_{k_3=1}^{M}A^{\xi}_{ik_1}A^{\eta}_{jk_2}A^{\eta}_{k_2k_3}w_{k_1k_3}\end{pmatrix}\\ &+(1-\upsilon)\lambda^3\left(B^{\eta}_{j1}\psi^{x}_{i1}+B^{\eta}_{jM}\psi^{x}_{iM}+\sum_{k_1=2}^{M-1}\sum_{k_2=1}^{N}B^{\eta}_{jk_1}A^{\xi}_{ik_2}w_{k_2k_1}\right)\\ \frac{V_y.a^3}{D}&=\lambda^3\left(B^{\eta}_{j1}\psi^{y}_{i1}+B^{\eta}_{jM}\psi^{y}_{iM}+\sum_{k_1=2}^{M-1}\sum_{k_2=1}^{M}B^{\eta}_{jk_1}A^{\eta}_{k_1k_2}w_{ik_2}\right)+\\ &\lambda\begin{pmatrix}\sum_{k1=1}^{M}A^{\xi}_{i1}A^{\eta}_{jk_1}\psi^{x}_{1k_1}+\sum_{k1=1}^{M}A^{\xi}_{iM}A^{\eta}_{jk_1}\psi^{x}_{Mk_1}\\ +\sum_{k_1=1}^{N-1}\sum_{k_2=1}^{M}\sum_{k_3=1}^{N}A^{\xi}_{ik_1}A^{\eta}_{jk_2}A^{\xi}_{k_2k_3}w_{k_3k_2}\end{pmatrix}\\ &+(1-\upsilon)\left(B^{\xi}_{i1}\psi^{y}_{1j}+B^{\xi}_{iN}\psi^{y}_{Nj}+\sum_{k_1=2}^{N-1}\sum_{k_2=1}^{M}B^{\xi}_{ik_1}A^{\eta}_{jk_2}w_{k_1k_2}\right)\end{aligned} \tag{29}$$

where, C^{ξ}_{ij} and B^{ξ}_{ij} are the weighting coefficients corresponding to the third and second order partial derivative to the ξ direction and C^{η}_{ij}, B^{η}_{ij} are those to the η direction.

4. Simulation of a crack in the refined DQEM

As it was mentioned earlier, the free vibration analysis of a thin plate with a central crack is impossible by using the conventional DQ or GDQ method. One way to overcome this problem is to use the Differential Quadrature Element Method (DQEM) (Striz *et al*.1994). In this method, a computational domain is divided into several subdomains (elements) which joined together mathematically by continuity conditions.

Hence, in order to simulate such a plate, a plate including a central crack of length b_2 is considered as depicted in Fig. 1. For implementing the EDQM, the pale surface divides into six elements so that the crack edges lies on the common side of the third and fourth elements (shown by the dashed line in Fig. 1).

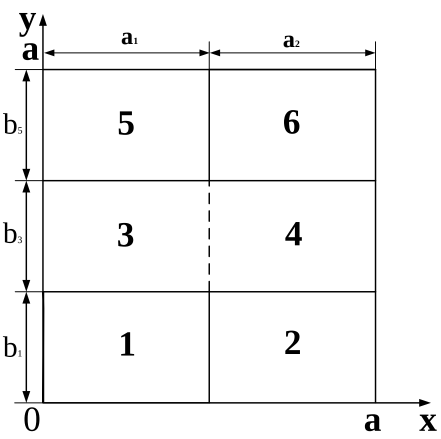

Fig. 1 Mesh grid of central cracked plate

It should be noted that the physical connection between the adjacent elements is provided by the compatibility conditions including continuity of transverse displacement, rotation, bending moments and shear forces. So, the continuity conditions can be expressed in y direction as follows

$$\begin{aligned} & w_q = w_l \\ & \Psi_q^y = \Psi_l^y \\ & \left(M_{yy}\right)_q = \left(M_{yy}\right)_l \\ & \left(V_{yy}\right)_q = \left(V_{yy}\right)_l \end{aligned} \quad , \ (\mathrm{q,l}) = \begin{pmatrix} 1,3 \\ 2,4 \\ 3,5 \\ 4,6 \end{pmatrix} \tag{30}$$

Also, in a similar manner the continuity conditions in x direction can be written as follows

$$\begin{aligned} & w_q = w_l \\ & \Psi_q^x = \Psi_l^x \\ & \left(M_{xx}\right)_q = \left(M_{xx}\right)_l \\ & \left(V_{xx}\right)_q = \left(V_{xx}\right)_l \end{aligned} \quad , \ (\mathrm{q,l}) = \begin{pmatrix} 1,2 \\ 5,6 \end{pmatrix} \tag{31}$$

where (q, l) indicates the common side of the qth and lth elements in the desired direction. However, because of the existence of free condition on the crack edges, the boundary conditions over that region are considered to be

$$\begin{aligned} & M_{xx}^{q} = 0 \\ & V_x^{q} = 0 \end{aligned} \quad , \quad q = \begin{pmatrix} 3 \\ 4 \end{pmatrix} \tag{32}$$

Also, the compatibility conditions at the crack tip, including continuity of vertical displacements, rotations, and the equilibrium of the bending moments, are porposed by

$$\begin{aligned} & w_q = w_l \qquad \Psi^x{}_q = \Psi^x{}_n \qquad \Psi^y{}_q = \Psi^y{}_l \\ & w_n = w_m \qquad \Psi^x{}_l = \Psi^x{}_m \qquad \Psi^y{}_n = \Psi^y{}_m \\ & w_q = w_n \qquad \Psi^x{}_q = \Psi^x{}_l \qquad \Psi^y{}_q = \Psi^y{}_n \\ & \left(M_{xx}\right)_q - \left(M_{xx}\right)_l + \left(M_{xx}\right)_n - \left(M_{xx}\right)_m = 0 \\ & \left(M_{yy}\right)_q + \left(M_{yy}\right)_l - \left(M_{yy}\right)_n - \left(M_{yy}\right)_m = 0 \\ & \left(M_{xy}\right)_q - \left(M_{xy}\right)_l - \left(M_{xy}\right)_n + \left(M_{xy}\right)_m = 0 \\ & \left(q,l,n,m\right) = \begin{pmatrix} 1,2,3,4 \\ 3,4,5,6 \end{pmatrix} \end{aligned} \tag{33}$$

where q, l, n and m represent the elements are around the cracked tips.

According to the aforementioned statements, Eq. (28) can be rewritten in the following form for the free vibration analysis of a discretized domain (See more details in Shu 2012)

$$\begin{aligned} & \left(C_{i1q}^{x}\psi_{1jq}^{x} + C_{iN_q q}^{x}\psi_{N_q jq}^{x} + \sum_{m=2}^{N_q-1}\sum_{n=1}^{N_q} C_{imq}^{x} A_{mnq}^{x} w_{njq} \right) + \\ & \lambda^4 \left(C_{j1q}^{y}\psi_{i1q}^{y} + C_{jM_q q}^{y}\psi_{iM_q q}^{y} + \sum_{m=2}^{M_q-1}\sum_{n=1}^{M_q} C_{jmq}^{y} A_{mnq}^{y} w_{inq} \right) \\ & + \lambda^2 \begin{pmatrix} \sum_{n=1}^{M_q} A_{i1q}^{x} B_{jnq}^{y} \psi_{1nq}^{x} + \sum_{n=1}^{M_q} A_{iN_q q}^{x} B_{jnq}^{y} \psi_{N_q nq}^{x} + \\ \sum_{m=2}^{N_q-1}\sum_{n=1}^{M_q}\sum_{k=1}^{N_q} A_{imq}^{x} B_{jnq}^{y} A_{mkq}^{x} w_{knq} \\ + \sum_{m=1}^{N_q} B_{imq}^{x} A_{j1q}^{y} \psi_{m1q}^{y} + \sum_{m=1}^{N_q} B_{imq}^{x} A_{jM_q q}^{y} \psi_{mM_q q}^{y} \\ + \sum_{m=1}^{N_q}\sum_{n=2}^{M_q-1}\sum_{k=1}^{M_q} B_{imq}^{x} A_{jnq}^{y} A_{nk}^{y} w_{mkq} \end{pmatrix} = \Omega^2 w_{ijq} \\ & \quad for \quad 2 \le i \le N_q - 1 \ , \ 2 \le j \le M_q - 1 \\ & \qquad and \quad q = 1,2,....,6 \end{aligned} \tag{34}$$

5. Boundary conditions

In this study, the boundary conditions of the cracked plate are considered to be simply supported on all edges.

At ξ=0:

$$w_q = 0 \quad \text{and} \quad M_q^{xx} = 0 \ , \ q = (1\ 3\ 5) \tag{35}$$

At ξ=1:

$$w_q = 0 \quad \text{and} \quad M_q^{xx} = 0, \quad q = (2\ 4\ 6) \tag{36}$$

At η=0:

$$w_q = 0 \quad \text{and} \quad M_q^{yy} = 0, \quad q = (1\ 2) \tag{37}$$

At η=1:

$$w_q = 0 \quad \text{and} \quad M_q^{yy} = 0, \quad q = (5\ 6) \tag{38}$$

The simply supported boundary conditions on the common nodes located on η=0 and η= 1 are

$$\begin{aligned} & w_q = w_l \qquad\qquad w_q = 0 \\ & \Psi^x{}_q = \Psi^x{}_l \qquad \Psi^x{}_q = 0 \\ & \Psi^y{}_q = \Psi^y{}_l \qquad \left(M_{yy}\right)_q + \left(M_{yy}\right)_l = 0 \end{aligned} \quad \left(q,l\right) = \begin{pmatrix} 1,2 \\ 5,6 \end{pmatrix} \tag{39}$$

Also, at ξ=0 and ξ=1, they can be written as follows

$$\begin{aligned} & w_q = w_l \qquad\qquad w_q = 0 \\ & \Psi^x{}_q = \Psi^x{}_l \qquad \Psi^y{}_q = 0 \\ & \Psi^y{}_q = \Psi^y{}_l \qquad \left(M_{xx}\right)_q + \left(M_{xx}\right)_l = 0 \end{aligned} \quad \left(q,l\right) = \begin{pmatrix} 1,3 \\ 2,4 \\ 3,5 \\ 4,6 \end{pmatrix} \tag{40}$$

At the corner points, the boundary conditions can be expressed by

$$\begin{aligned} & w_q = 0 \\ & \psi_q{}^x = 0 \quad q = 1,2,5,6 \\ & \psi_q{}^y = 0 \end{aligned} \tag{41}$$

In other words, at the edges of a classical plate having simply supported boundary conditions, the slope and its derivatives are zero. In order to explain more, $\frac{\partial^2 w}{\partial y^2}$ equal to zero at an edge with simply supported boundary conditions at ξ=0 or ξ=1, respectively. With regard to this issue, Eq. (25) can be expressed by

$$A_{j1}^{y}\psi_{i1}^{y}+A_{jM}^{y}\psi_{iM}^{y}=0 \tag{42}$$

It can be seen that the trivial solution of this equation is zero.

6. Solution methodology

The combination of the aforementioned discretized governing equations and the associated boundary condition equations can be represented by a system of linear equations through an assembling procedure so that the continuity conditions between adjacent DQ elements are satisfied (See more details in Navardi 2015).

$$\begin{bmatrix} K_{BB} & K_{BD} \\ K_{DB} & K_{DD} \end{bmatrix}\begin{bmatrix} \delta_B \\ \delta_D \end{bmatrix}-\Omega^2\begin{bmatrix} 0 \\ \delta_D \end{bmatrix}=\begin{bmatrix} 0 \\ 0 \end{bmatrix} \tag{43}$$

$$\delta_B=\begin{pmatrix} \{w\}_B \\ \{\psi^x\}_B \\ \{\psi^y\}_B \end{pmatrix} \tag{44}$$

where the subscripts B and D denote the boundary and interior points along the domain, respectively. K_{BB}, K_{BD}, K_{DB} and K_{DD}imply the influence coefficients appeared in the discretized equations. δ_B is the degree of freedom vector including transverse displacements and slope states which considered on the boundaries of domain and defined by:

Also, δ_D is the degree freedom vector including transverse displacement of the interior points along a domain and defined by

$$\delta_D=\{w\}_D \tag{45}$$

Computing δ_B from the first row of Eq. (43) and substituting it into its second row results in the following relation.

$$K\delta_D=\Omega^2\delta_D \tag{46}$$

where

$$\begin{aligned} \delta_B &= -K_{BB}^{-1}K_{BD}\delta_D \\ K &= K_{DD}-K_{DB}K_{BB}^{-1}K_{BD} \end{aligned} \tag{47}$$

The eigen-frequencies of Eq. (47) can be determined through a standard eigenvalue solver.

7. Results and discussion

In this section, in order to validate the present approach, two test cases including a square thin plate with a central crack and a square thin plate with a side crack are investigated by the refined DEQM. The results are validated by those obtained via FEM and available results in the literature.

Table 1 The first nine non-dimensional natural frequencies of a square plate with a central crack

Frequency	FEM[2]	Ref.[2]	Grid point numbers in each element			
			18	22	26	30
Ω_1	16.397	16.41	16.5889	16.3101	16.2592	16.2406
Ω_2	27.703	27.77	28.0030	27.8095	27.7047	27.6418
Ω_3	47.179	47.21	46.8498	46.8946	46.9217	46.9387
Ω_4	65.642	65.76	62.3396	62.3513	62.3125	62.2732
Ω_5	76.297	76.37	77.0309	76.3710	76.2417	76.1917
Ω_6	78.308	-	78.23887	78.152	78.1088	78.0835
Ω_7	96.702	-	97.03991	96.5751	96.4934	96.4647
Ω_8	113.338	-	113.0641	113.047	113.038	113.0328
Ω_9	121.207	-	122.2504	121.854	121.646	121.524

Table 2 The first five non-dimensional natural frequencies of a square plate with side crack

Frequen-cy	FEM	Grid point numbers of each rear element in *y* direction						
		10	14	16	17	20	22	24
Ω_1	17.832	27	17.5394	17.8081	17.8680	17.1515	16.8730	16.3651
Ω_2	40.339	35.1634	40.7690	41.1847	41.1517	41.5708	42.1345	43.6626
Ω_3	46.020	35.1634	44.9926	46.7988	47.1076	44.9404	44.7239	44.0295
Ω_4	62.118	56.5341	61.4402	61.4810	61.3314	60.1237	58.7240	57.3540
Ω_5	72.902	56.5341	73.4507	73.7366	73.7582	73.5844	73.6852	73.6831

7.1 Free vibration analysis of a square thin plate with a central crack

A thin plate with a central crack and under simply supported boundary conditions is considered here and it is divided into six elements as shown in Fig. 1. By using the present approach, the first nine dimensionless natural frequencies of a cracked thin plate have been determined and presented in Table 1.

In this table, the convergence of the results is shown by the use of a different number of grid points. Also, the obtained results are compared with those reported by Huang *et al.* (2011). It should be noted that they utilized the Ritz method and FEM to the free vibration analysis of a cracked plate. Also, the maximum percentage error is less than 5 percent. The results reveal that the present approach gives satisfactory results in comparison with FEM and analytical methods. Also, the related mode shapes of that plate obtained by the present approach are illustrated in Fig. 2.

The effect of crack length on the non-dimensional natural frequencies of the plate is shown in Fig. 3. Indeed, Ansys software has been utilized to investigate the validation of the obtained results. For this purpose, Solid185 was used for 3D modeling of the cracked plate. Also, the location of the crack tip (a_1) is considered to be 0.2 in all cases. There is a good correlation between the present approach and FEM. It must be noted that a sampling point distribution including 15×15 grid points in each element is considered here

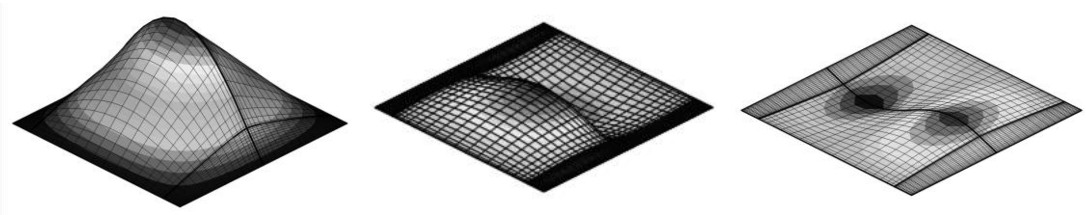

(a) 1st mode (b) 2st mode (c) 3st mode

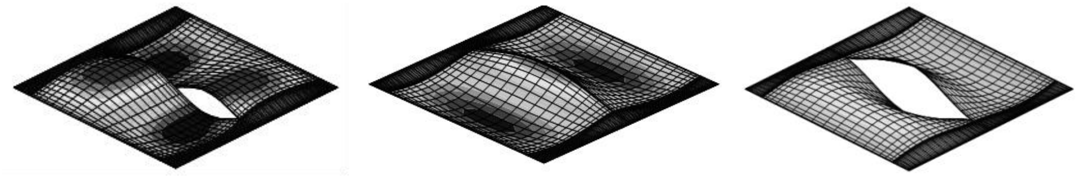

(d) 4st mode (e) 5st mode (f) 6st mode

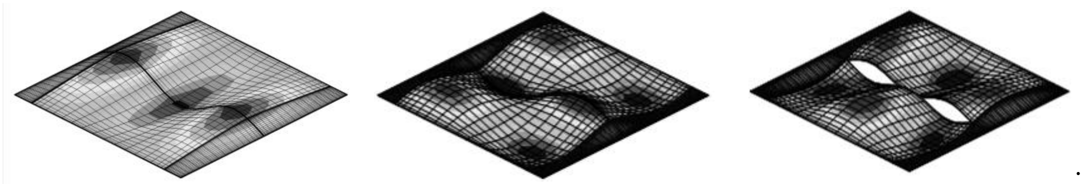

(g) 7st mode (h) 8st mode (i) 9st mode

Fig. 2 The first nine mode shapes of a square plate with a central crack

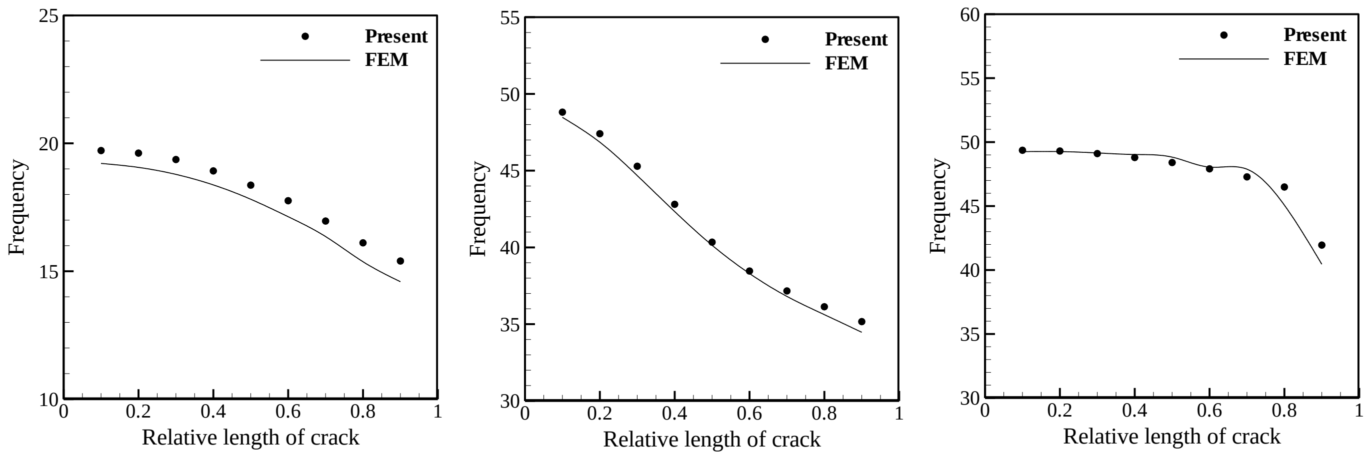

(a) 1st mode (b) 2st mode (c) 3st mode

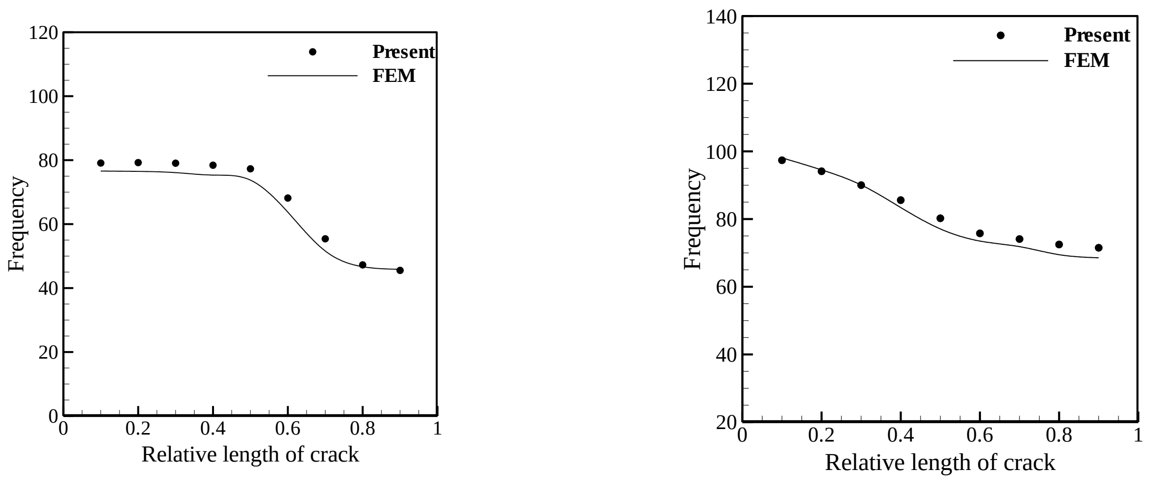

(d) 4st mode (e) 5st mode

Fig. 3 Effect of crack length on the frequencies of a square plate with a central crack

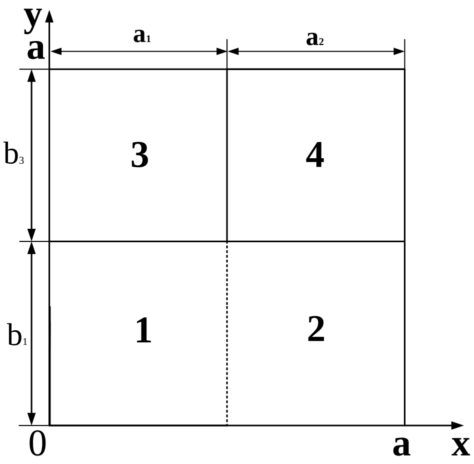

Fig. 4 Mesh grid of a plate with a side crack using four elements

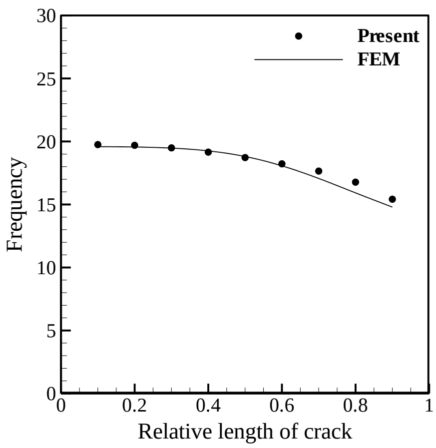

(a) 1st mode

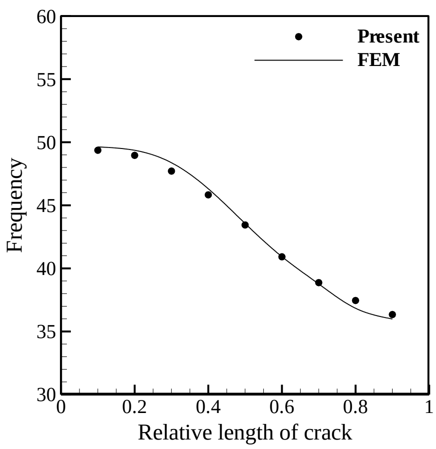

(b) 2st mode

Fig. 5 Effect of crack length on the frequencies of a square plate with a side crack

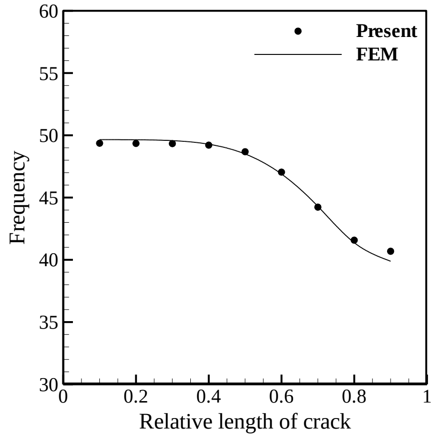

(c) 3st mode

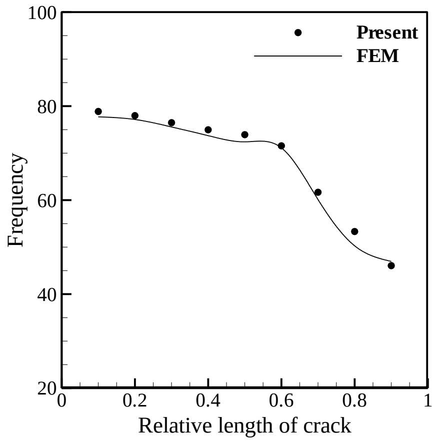

(d) 4st mode

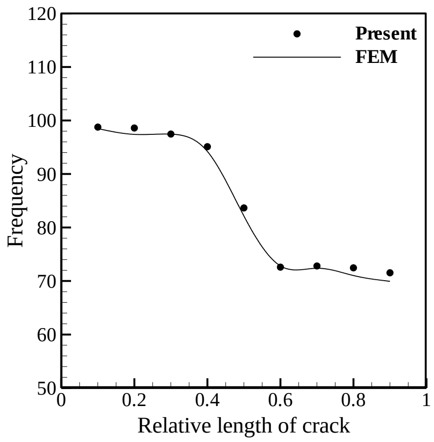

(e) 5st mode

Fig. 5 Continued

7.2 Free vibration analysis of a square thin plate with a side crack

Here, the results of the free vibration analysis of a square plate with a side crack are presented by using the present method. For this purpose, the plate is divided into four elements (as shown in Fig. 4) and a sampling point distribution including 15×15 grid points in each element adjacent to the crack edges is considered. The crack location is illustrated by the dotted line in this figure.

Table 2 indicates the first five non-dimensional natural frequencies of a thin cracked plate by the present method and FEM. The geometric specifications of the side crack have been defined by $\frac{b_3}{b}=0.6$ and $\frac{a_1}{a}=0.2$. The related FE models have been constructed using the previously mentioned element in Ansys software. The effect of a number of grid points in the y direction which considered on the elements behind of the crack tip on the convergence of the results is studied and presented in this table. It must be noted that the number of grid points is 15 in the x direction inside each element. This subject reveals that the importance of the number of computational nodes on the results because of asymmetry of the whole computational domain (the cracked plate).

According to the results, it is found that the results are affected by the number of computational points which located behind the crack tip. So, the correct answer can be achieved when the number of points considered along the edgewise orientation (y direction) in each rear element is (16 points) higher than those in the direction perpendicular to the edge of the crack (15 points). Of course, using of more computational nodes results in incorrect answer due to computational problems.

Finally, Fig. 5 shows the effect of the crack length on the first five non-dimensional natural frequencies of the cracked thin plate. Also, it is shown that the obtained results have a good correlation with those obtained by FEM.

The results show that the natural frequencies decrease with increasing the crack length because of increasing flexibility of the plate.

8. Conclusions

In this study, a refined approach in the generalized differential quadrature element method has been proposed to provide the free vibration analysis of cracked thin plate structures. The framework of this study was established based on the classical plate theory. Thus, the main feature of this approach is to refine the GDQ formulation based on the classical plate theory through incorporating an additional degree of freedom. Also, an appropriate form of continuity equations has been proposed to model a crack tip which surrounded by some DQ elements. To show the accuracy and fidelity of the present approach, the free vibration analyses of some different test cases including a square thin plate with a central crack and the other with a side crack under simply supported boundary conditions were conducted. The evaluation of the obtained results clarifies the accuracy and convergence of the present method. However, it was found that for analyzing a plate with a side crack, one can need more computational points in the crack edgewise, in the elements located behind the crack tip, to achieve acceptable results.

References

Bachene, M., Tiberkak, R. and Rechak, S. (2009), "Vibration analysis of cracked Plates Using the Extended finite element method", *Arch. Appl. Mech.*, **79**, 249-262.

Barooti, M. (2013), "Stability analysis of symmetric orthotropic composite plates with through the width delamination", MSc Thesis, Amirkabir University of Technology University, Tehran, Iran.

Bellman, R and Casti, J. (1971), "Differential quadrature and long-term integration", *J. Math. Anal. Appl.*, **34**, 235-238.

Bose, T. and Mohanty, A.R. (2013), "Vibration analysis of a rectangular thin isotropic plate with a part-through surface crack of arbitrary orientation and position", *J. Sound Vib.*, **332**, 7123-7141.

Chen, W., Zhong, T.X. and Liang, S.P. (1997), "On the DQ analysis of geometrically non-linear vibration of immovably simply-supported beams", *J. Sound Vib.*, **206**, 745-748.

Chen, W., Zhong, T.X. and Shu, C. (2002), "A Lyapunov formulation for efficient solution of the poisson and convection-diffusion equations by the differential quadrature method", *J. Comput. Phys.*, **141**, 78-84.

Fantuzzi, N. (2013), "Generalized differential quadrature finite element method applied to advanced structural mechanics", Ph.D. Dissertation, University of Bologna , Bologna, Italy.

Fantuzzi, N., Tornabene, F. and Viola, E. (2014), "Generalized differential quadrature finite element method for vibration analysis of arbitrarily shaped membranes", *Int. J. Mech. Sci.*, **79**, 216-251.

Han, J.B. and Liew, K. (1996), "The differential quadrature element method (DQEM) for axisymmetric bending of thick circular plates", *The Third Asian-Pacific Conference on Computational Mechanics*, Seoul, September.

Hsu, M.H. (2005), "Vibration analysis of edge-cracked beam on elastic foundation with axial loading using the differential quadrature method", *Comput. Meth. Appl. Mech. Eng.*, **194**, 1-17.

Huang, C.S. and Leissa, A.W. (2009), "Vibration analysis of rectangular plates with side cracks via the Ritz method", *J. Sound Vib.*, **323**, 974-988.

Huang, C.S., Leissa, A.W. and Chan, C.W. (2011), "Vibrations of rectangular plates with internal cracks or slits", *Int. J. Mech. Sci.*, **53,** 436-445.

Israr, A. (2008), "Vibration analysis of cracked aluminum plates", Ph.D. Dissertation, University of Glasgow.

Karami, G. and Malekzadeh, P. (2003), "Application of a new differential quadrature methodology for free vibration analysis of plates", *Int. J. Numer. Meth. Eng.*, **56**, 847-868.

Ke, L., Wang, Y. and Yang, J. (2012), "Nonlinear vibration of edged cracked FGM beams using differential quadrature method", *Sci. China Phys. Mech. Astron.*, **55,** 2114-2121.

Leissa, A.W. (1973), "The free vibration of rectangular plates", *J. Sound Vib.*, **31**, 257-293.

Liu, F.L. (2001), "Differential quadrature element method for buckling analysis of rectangular Mindlin plates having discontinuities", *Int. J. Solid. Struct.*, **38**, 2305-2321.

Liu, F.L. and Liew, K. (1998), "Static analysis of Reissner-Mindlin plates by differential quadrature element method", *J. Appl. Mech.*, **65**,705-710.

Liu, F.L. and Liew, K. (1999), "Differential quadrature element method for static analysis of Reissner–Mindlin polar plates", *Int. J. Solid. Struct.*, **36**, 5101-5123.

Liu, F.L. and Liew, K. (1999), "Differential quadrature element method: a new approach for free vibration analysis of polar Mindlin plates having discontinuities", *Comput. Meth. Appl. Mech. Eng.*, **179**, 407-423.

Liu, F.L. and Liew, K. (1999), "Vibration analysis of discontinuous Mindlin plates by differential quadrature element method", *J. Vib. Acoust.*, **121**, 204-208.

Navardi, M.M. (2015), "Supersonic flutter analysis of thin cracked plate by Differential Quadrature Method", MSc Thesis, Amirkabir University of Technology University, Tehran, Iran.

Reddy, J.N. (2004), *Mechanics Of Laminated Composite Plates And Shells: Theory and Analysis*, CRC press, London, British.

Shu, C. (2012), *Differential Quadrature And Its Application In Engineering*, Springer, London, British.

Shu, C. and Richards, B.E. (1992), "Application of generalized differential quadrature to solve two-dimensional incompressible Navier-Stokes equations", *Int. J. Numer. Meth. Fluid.*, **15**, 791-798.

Striz, A.G., Weilong, C. and Bert, C.W. (1994), "Static analysis of structures by the quadrature element method (QEM)", *Int. J. Solid. Struct.*, **31**, 2807-2818.

Torabi, K., Afshari, H. and Aboutalebi, F.H. (2014), "A DQEM for transverse vibration analysis of multiple cracked non-uniform Timoshenko beams with general boundary conditions", *Comput. Math. Appl.*, **67**, 527-541.

Viola, E., Tornabene. F. and Fantuzzi, N. (2013), "Generalized differential quadrature finite element method for cracked composite structures of arbitrary shape", *Compos. Struct.*, **106**, 815-834.

Wang, Y., Wang, X. and Zhou, Y. (2004), "Static and free vibration analyses of rectangular plates by the new version of the differential quadrature element method", *Int. J. Numer. Meth. Eng.*, **59**, 1207-1226.

Wu, T. and Liu, G. (2001), "The generalized differential quadrature rule for fourth-order differential equations", *Int. J. Numer. Meth. Eng.*, **50**, 1907-1929.

Zong, Z. and Zhang, Y. (2009), *Advanced Differential Quadrature Methods*, CRC Press, New York, NY, USA.

PL